ISSN Print: 2394-7500
ISSN Online: 2394-5869
Impact Factor: 8.4
IJAR 2022; 8(8): 340-347
www.allresearchjournal.com
Received: 14-05-2022
Accepted: 23-06-2022

Suram Singh
Department of Chemistry, Govt. Degree College, Billawar, Jammu and Kashmir, India

Roshan Lal
Department of Chemistry, Govt. Degree College Kathua (Boys), Jammu and Kashmir, India

Corresponding Author:
Suram Singh
Department of Chemistry, Govt. Degree College, Billawar, Jammu and Kashmir, India

Physical properties of perovskite-type Lanthanum ferrites used as energy material in solid oxide fuel cells

Suram Singh and Roshan Lal

Abstract
In this paper synthesis of perovskite-type Lanthanum ferrites material which is done by soft chemical method using an organic combustion fuel is reported. The aim of this study is to evaluate the physical properties of Lanthanum ferrites material. Structural characterizations of the material were carried out by X-ray diffraction technique which revealed that the synthesized nano-structure was single phase with orthorhombic symmetry. The mean crystallite size of the sample was calculated by Scherer's formula. Nano-sized Lanthanum ferrites material with specific surface area in the range of 18.3 m^2/g and crystallite size in the range of 59 nm was obtained. The surface morphology examination was carried out by Scanning electron microscope. Transmission Electron Microscope investigations reveal that nano-materials with particle size in the range of 46 to 56 nm were obtained. The nano-size material synthesized by soft-chemistry combustion method showed better magnetic properties for applications as soft magnetic devices used in solid oxide fuel cells.

Keywords: Nano-materials, lanthanum ferrites, wet chemical method, rietveld refinements, SEM analysis

1. Introduction
Surface and particle size effects in nano-scale materials have been the subject of growing interest in recent years. As the particle size decreases, an increasing fraction of atoms lie at or near the surface and then surface and interface effects become more and more important. Nano-scale materials have attracted extensive attention as a result of their novel size-dependent properties. Nano-materials exhibit different physical and chemical properties compared to their bulk materials. It is well known that by controlling the size of the particles it is possible to tune their properties. Most of the research efforts which were concentrated on the mixed metal oxides of the perovskite family, particularly lanthanum ferrites are important in advanced technologies such as solid oxide fuel cells, photo catalysis, gas sensors and memory storage devices [1-5]. One of most common perovskite oxides, Lanthanum ferrite nano-crystal is a very known material and thus has received intensive investigations over years [6, 7].
The most prominent and conventional way of preparing these materials is by solid-state reaction, which involves the mixing of the corresponding oxides/carbonates with extensive mechanical grinding followed by sintering at very high temperature. These rigorous conditions lead to bulk materials, which may or may not exhibit a nano-crystalline structure. In addition, this technique has also several problems such as high reaction temperature, poor homogeneity, high porosity and poor control of the particle size, which indirectly affects the functional properties of the materials. On the other hand, the soft-chemical techniques such as sol–gel, co-precipitation, citrate-gel and combustion synthesis methods yield nano-sized materials with good homogeneity, low porosity and good control over particle size [8-12]. In this context, we have investigated and synthesised nano-sized Lanthanum ferrites material by soft-chemical technique using an organic combustion fuel.

2. Experimental
Nano-crystalline sample of Lanthanum ferrites were prepared by soft chemical technique using an organic combustion fuel. The A.R grade lanthanum nitrate, iron nitrate along with an organic fuel were used as the starting ingredients. Synthesis was carried at room temperature without protecting by any inert gases.

The combustion ratio of oxidizer (O) which is metal nitrate and fuel (F) that is Φ_e (O/F) was calculated using the total valence of oxidizers (metal nitrates) and the reducing valence of the fuel according to the principle of propellant chemistry [13]. When Φe becomes unity, it serves as the maximum heat release at the time of combustion. The oxidizing and reducing valencies of various elements involved in the stoichiometry of the redox mixture for combustion were calculated by following the methods available in the recent literature [14]. Thus, stoichiometric amounts of reactant species were mixed together thoroughly in an agate mortar and pestle to get a homogeneous mixture. The slurry substance was formed due to the hygroscopic nature of metal nitrates. In the combustion process, firstly the slurry undergoes dehydration at 60 ºC followed by spontaneous combustion at 200 ºC with the evolution of voluminous gases yielding a voluminous and foamy product. The entire combustion reaction was completed within few minutes. The foamy powder was then heated in static air at 450 ºC for one and half hour in the muffle furnace to obtained the fine sample of Lanthanum ferrite.

The phase composition of the obtained samples was characterized by using X'Pert PRO ALPHA1 of Panalytical diffractometer equipped with Ni-filtered CuKα radiations operated at 45 kV and 40 mA. X-ray diffraction measurements were carried out at room temperature in the 2θ scanning range from 20° to 100° with a step size of 0.0171° and continuous scan step time of 21s. The structural parameters were determined for the desired sample by means of the Rietveld refinement method using the *GSAS* software [15]. The average crystallite size was calculated using XRD data, using Debye-Scherrer's formula [16].

The microstructures of the nano-sample were examined by scanning electron microscope FE-SEM Quanta 200 FEG with an accelerating voltage of 200V–30 kV. Energy-dispersive X-ray analysis (EDS) spectra were measured on a JEOL-JSM-840 scanning microscope using INCA attachment with the SEM instrument. The particle size of the nanopowders was determined by transmission electron microscope (TEM, Model; Technai G2 20 S-TWIN FEI Netherlands). Samples for TEM analysis were prepared by placing a drop of the powder sample suspension after treated with oscillation thoroughly on a carbon-coated copper TEM grid, allowing it to dry in air and analyzed at an accelerating voltage of 20kV-200kV.

The magnetic properties were investigated by means of magnetization measurements obtained using Faraday magnetic balance, provided with Polytronic made electromagnet within the temperature range 85-300 K under a static applied magnetic field of 0.25T.

3. Results and discussion

Powder X-ray diffraction patterns of the Lanthanum ferrite nano-powders successfully prepared by combustion reaction method are shown in Fig.1. The X-ray diffraction pattern shows peaks corresponding to the Lanthanum ferrites pattern without traces of other phases. Assuming spherical shape grains, an average size of 59 nm was obtained from the X-ray diffraction line using the Scherrer equation. Such a value is in agreement with transmission electron microscopy (TEM) measurements showing nano-powders with diameter in the range 46-56 nm.

The nanopowders so obtained are monophasic and can be indexed to an orthorhombic structure with the space group, *Pbnm*, in which La at 4c (*x*, *y*, 0.25), Fe at 4b (0, 0.5, 0), O(1) at 4c (*x*, *y*, 0.25) and O(2) at 8d (*x*, *y*, *z*). The average grain size, determined by Debye-Scherrer's formula, is found to be in the range of 59 nm. The structural parameters are refined by the Rietveld method using the *GSAS* software. There is a close match between observed and calculated patterns as shown in Fig. 2. The refined structural parameters *viz*;, the residuals for the weighted pattern R_{wp}, the pattern R_p, structure factor R_F, and goodness of fit χ_2 are listed in Table 1.

The average grain size (T_G) of the sample was determined by Debye–Scherrer's formula [16]:

$$T_G = \frac{0.9\lambda}{\beta cos\theta}$$

where λ is the X-ray wavelength used, θ is the diffraction angle for the most intense peak (112) and β_2 is defined as $\beta_2 = \beta_{m2} - \beta_{s2}$. Here β_m is the experimental full width at half maximum (FWHM) and β_s is the FWHM of the as-prepared sample.

In order to determine the elemental analysis and confirm that there is no loss of any integrated element after sintering, energy dispersive X-ray analysis (EDX) were carried out parallel to the SEM analysis. The analysis of the chemical elements has been done on two different regions. A typical cationic composition has been calculated from the averages of mass percentage of these two regions of sample heated at 450ºC. Elemental analysis (mass%) of La, Fe and O calculated from EDX spectrum is provided in Table 2, while energy dispersive X-ray spectrum is given in Fig. 3. It can be seen that the experimental values are in good agreement with the theoretical values.

The particle size and surface morphology of the nano powders were examined by TEM and SEM micrographs are shown in Fig. 4 & Fig. 5 respectively. The nano-sample consists of highly agglomerated grains and is composed of porous networks, which is due to the evaluation of a large amount of gases during charring. Part of the powder agglomerates to become sponge-like and the particles tend to fuse together to form network-like structure, as seen in Fig. 4. The TEM pictures of the as-burnt powder and powder heated at 450 °C are also shown in Fig. 5. Similar to the SEM observation, the particles on TEM images are also agglomerated. However, the grain boundaries are clearly distinguishable. It can be seen from TEM micrograph (Fig. 5) that the diameter of particle size is in the range of about 46 to 56 nm.

By assuming that the Lanthanum ferrite powder is consists of spherical grains, the specific surface area can be calculated using equation [17-20].

$$S = \frac{6000}{d.\mathrm{TG}}$$

where *d* is X-ray density and T_G is the average grain size in nm and its values are given in Table 3.

Fig. 6 shows the temperature dependence of the magnetization, *M (T)* measurements for lanthanum ferrite materials under zero-field-cooled (ZFC) conditions. The magnetic susceptibility of the sample decreases with rise in temperature and hence thereby increases with decreasing particle size. Yan *et al*. [21] found that the magnetic susceptibility of their samples increased as the surface-to-

volume ratio increased and attributed this to localized spins on the surface of the material. Harada *et al.* [22] found similar results; the magnetization increased with decreasing particle size and they suggested the source to be chemisorption of oxygen atoms at the surface. Fig. 7 shows the temperature dependence of the inverse magnetic susceptibility for lanthanum ferrites. The magnetic susceptibility obey Curie-Weiss law over the whole temperature range studied from 90-295 K where the samples behave like a normal paramagnet. The Curie-Weiss temperature (Θ) is negative for all the samples indicating the presence of anti-ferromagnetic interactions in them. By fitting the linear paramagnetic region of the data, the Curie-Weiss parameters C and Θ were obtained. The experimental effective paramagnetic moments (μ_{eff}) were calculated from the relation: $\mu_{eff} = 2.828\sqrt{C}$ and the values of μ_{eff} and Θ are given in Table 3. It has been observed that magnetic moment increases with decreasing particle size. The magnetic moment of the anti-ferromagnetic lanthanum ferrite nanoparticles originate from the spin uncompensation at the surface [23]. As the particle size decreases, an increasing fraction of atoms lie at or near the surface and then the spin un-compensation increases. Hence, the moment of an anti-ferromagnetic particle is expected to increase significantly with decreasing particle size. In this context, anti-ferromagnetic nano-particles have recently been the subject of renewed attention due to their enhanced surface and interface effects, because of the much lower core moment with respect to ferromagnetic particles of the same size. Because of spin uncompensation at the surface, the particle moment of an anti-ferromagnetic particle is expected to increase significantly with decreasing particle size. Moreover, there can be core moment uncompensation, as shown by atomic-scale modeling of lanthanum ferrite nano-particles.

Table 1: Structural parameters of lanthanum ferrite nano-sample obtained from the Rietveld refinement of X-ray diffraction patterns. The atomic sites are: La 4c[*x*, *y*, 0.25]; Fe 4b[0, 0.5, 0]; O(1) 4c[*x*, *y*, 0.25]; O(2) 8d[*x*, *y*, *z*] in the space group *Pbnm*.

a (Å)		5.5576(15)
b (Å)		5.5538(14)
c (Å)		7.8383(11)
V (Å^3)		241.94(10)
d (*g cm*$^{-3}$)		6.664
x	La	-0.0035(5)
	O(1)	0.062(4)
	O(2)	0.7311(18)
y	La	0.0244(5)
	O(1)	0.483(4)
	O(2)	0.2869(18)
z	O(2)	0.0442(18)
U_{iso} (Å^2)	La	0.02176(6)
	Fe	0.01515(8)
	O(1)	0.08202(7)
	O(2)	0.03314(4)
R_{wp}		0.1324
R_p		0.0983
χ^2		1.294

Table 2: EDX results of lanthanum ferrite nano-sample.

Element	Experimental mass%	Theoretical mass%
La	55.15	57.22
Fe	23.37	23.00
O	21.48	19.77

Table 3: Average grain size (T_G), X-ray density (d), specific surface area (S), Weiss constant (Θ) and effective magnetic moment (μ_{eff}) of lanthanum ferrite nano-powder.

T_G (nm)	d (g/cm^3)	S (m^2/g)	Θ (K)	μ_{eff} (B.M.)
59	5.84	18.3	–256	3.74

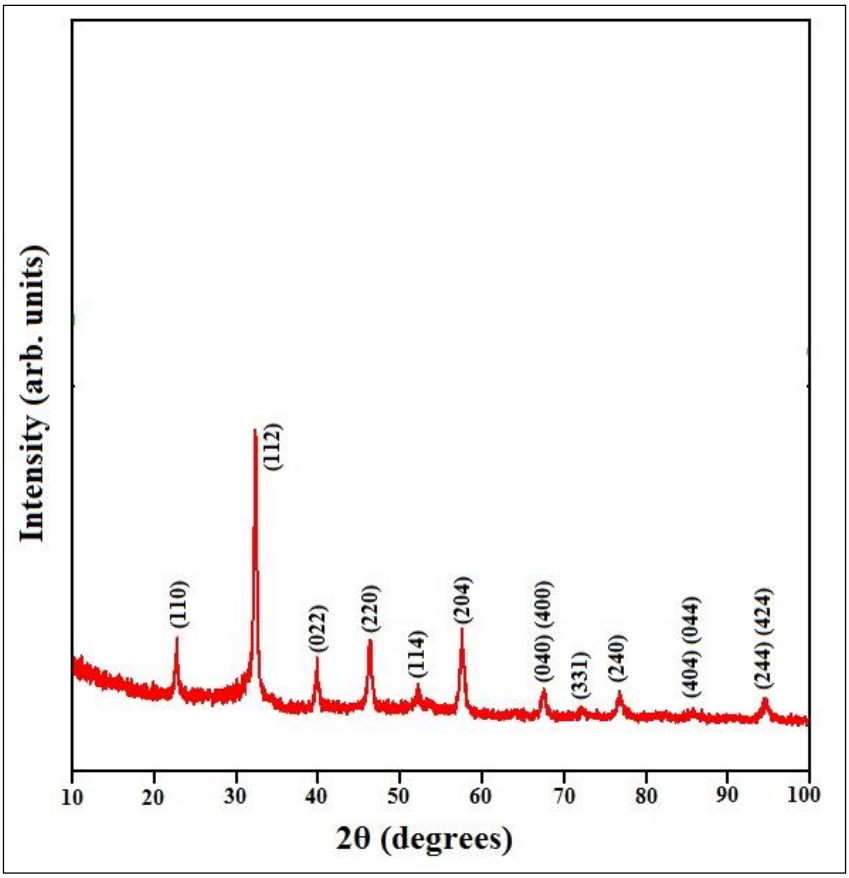

Fig 1: X-ray diffraction patterns of lanthanum ferrite nano-sample

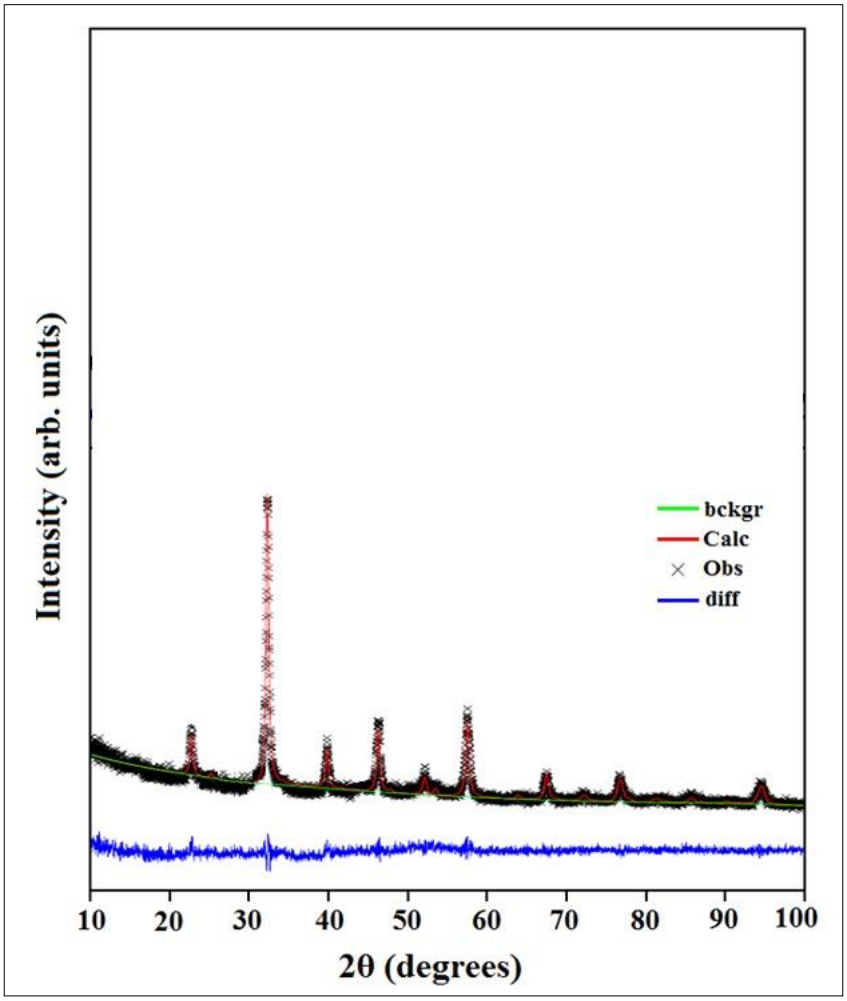

Fig 2: Rietveld refinement profile of lanthanum ferrite nano-sample

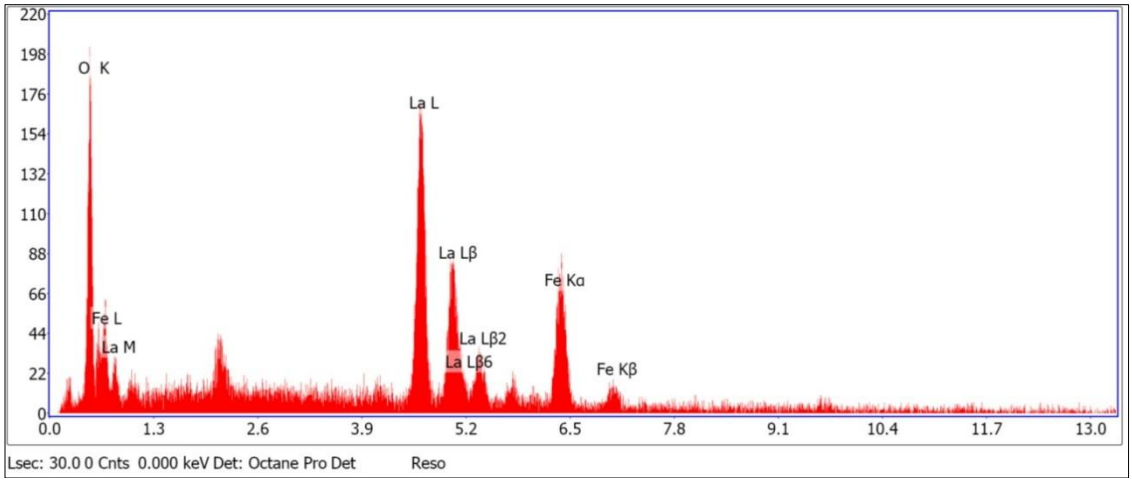

Fig 3: EDX spectrum of lanthanum ferrite nano-sample

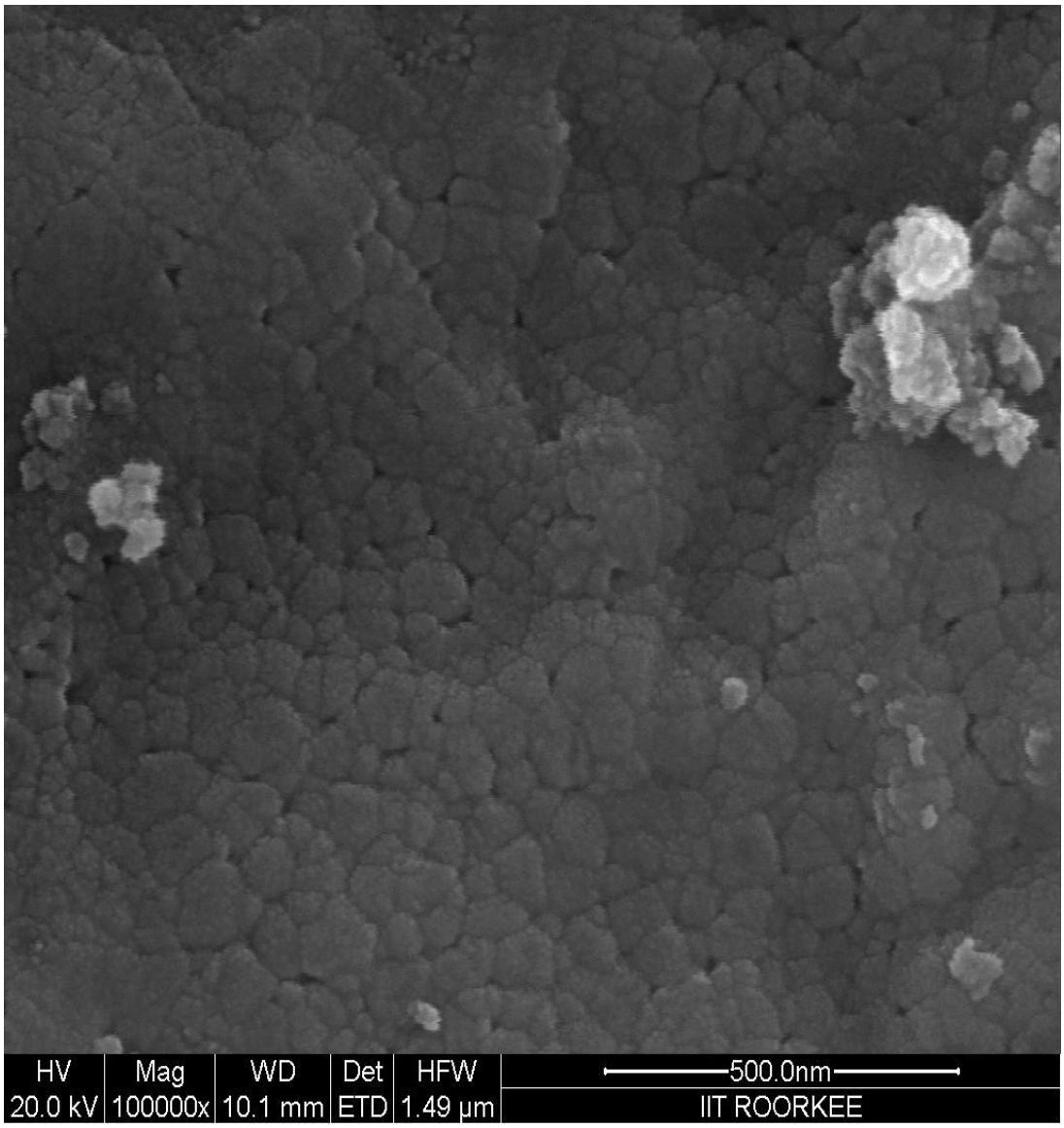

Fig 4: SEM micrograph of lanthanum ferrite nano-sample

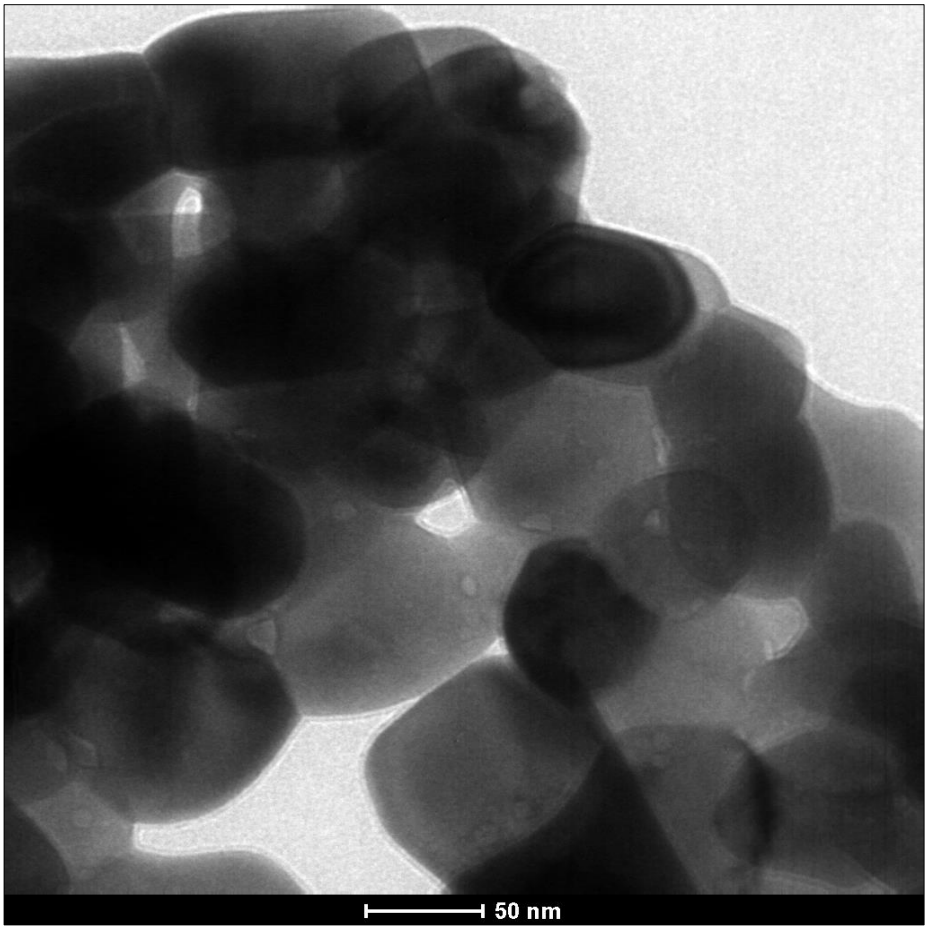

Fig 5: TEM micrographs of lanthanum ferrite nano-sample

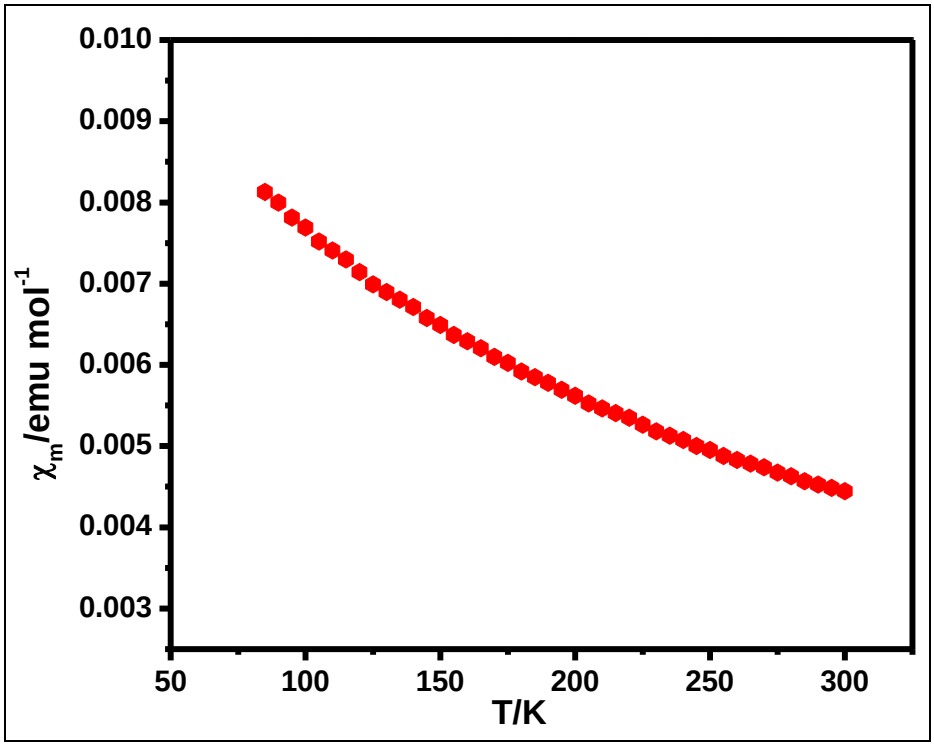

Fig 6: Plot of magnetic susceptibility (χ_m) versus temperature of lanthanum ferrite nano-sample

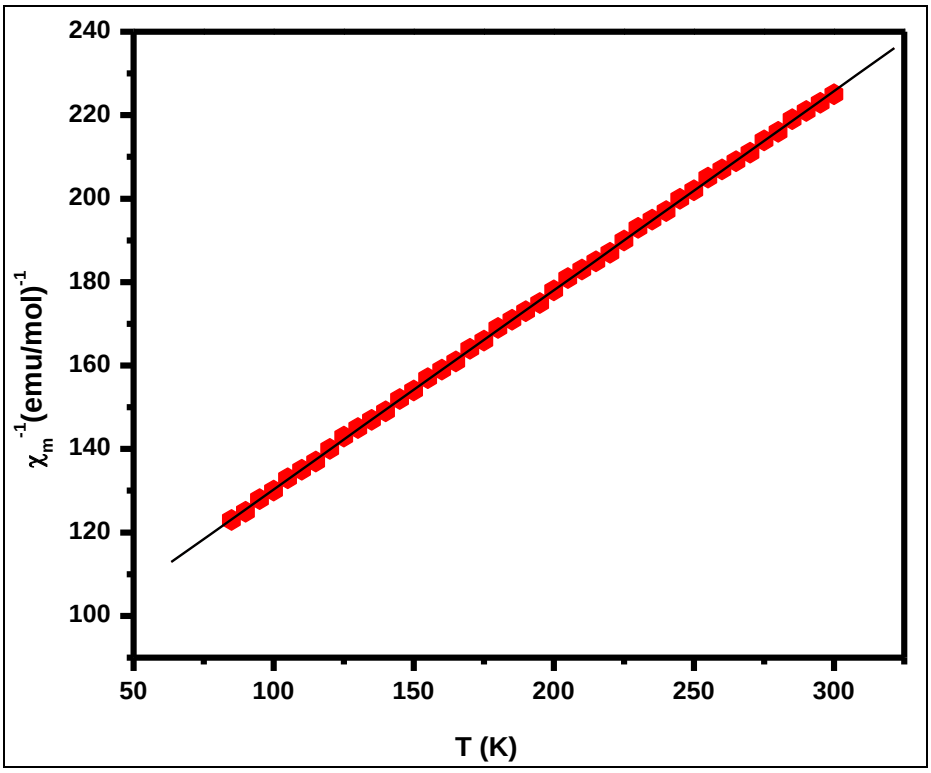

Fig. 7: Plot of inverse molar magnetic susceptibility (χ_m^{-1}) versus temperature of lanthanum ferrite nano-sample

4. Conclusion

Lanthanum ferrite nano-sample was prepared by soft chemical method using an organic combustion fuel. Rietveld refinements show that the nano-sample crystallize with orthorhombic unit cell in the space group *Pbnm*. A pure nano-sized lanthanum ferrite powder with specific surface area of 18.3 m^2/g and a crystallite size of 59 nm was obtained, while TEM investigations reveal a porous powder with particles diameter in the range of 46 to 56 nm. The Weiss constant (Θ) is negative for the lanthanum ferrite sample, indicating the presence of antiferromagnetic interactions in them.

5. Acknowledgements

Authors are also thankful to Dr. Harpreet Singh, Central Research Facility Section, Indian Institute of Technology Ropar, for recording XRD. Thanks are also due to Prof. Ramesh Chandra, Institute Instrumentation Centre, Indian Institute of Technology, Roorkee, for recording EDX, SEM and TEM.

6. References

4. Ding J, Lü X, Shu H, Xie J. Zhang H. Microwave-assisted synthesis of perovskite $ReFeO_3$ (Re: La, Sm, Eu, Gd) photocatalyst. Mater Sci and Engr B. 2010 Jul 25;171(1-3):31-4.
5. Sivakumar M, Gedanken A, Bhattacharya D, Brukental I, Yeshurun Y, Zhong W, *et al*. Sonochemical Synthesis of Nanocrystalline Rare Earth Orthoferrites Using $Fe(CO)_5$ Precursor. Chem. Mater. 2004 Sep 21;16(19):3623-32.
6. Wu AH, Shen H, Xu J, Jiang LW, Luo LQ, Yuan SJ, *et al*. Preparation and magnetic properties of $RFeO_3$ nanocrystalline powders. J. Sol-Gel Sci. Technol. 2011 Jul;59(1):158-63.
7. Winkler E, Zysler RD, Mansilla MV, Fiorani D. Surface anisotropy effects in NiO nanoparticles, Phys. Rev B. 2005 Oct 21;72(13):132409.
8. Wang D, Chu XF, Gong ML. Single-crystalline $LaFeO_3$ nanotubes with rough tube walls: synthesis and gas-sensing properties, Nanotechnology 2006 Oct 20;17(21):5501-5505.
9. Martinelli G, Carotta MC, Ferroni M, Sadaoka Y, Traversa E. Screen-printed perovskite-type thick films as gas sensors for environmental monitoring. Sens Actuators B. 1999;55(2-3):99-110.
10. Seo JW, Fullerton EE, Nolting F, Scholl A, Fompeyrine J, Locquet J-P. Antiferromagnetic $LaFeO_3$ thin films and their effect on exchange bias. J. Phys. Condens. Matter. 2008;20(26):264014-264024.
11. Phokha S, Pinitsoontorn S, Maensiri S, Rujirawat S. Structure, optical and magnetic properties of $LaFeO_3$ nanoparticles prepared by polymerized complex method, J Sol-Gel Sci Technol. 2014 Aug;71(2):333-41. DOI 10.1007/s10971-014-3383-8
12. Thuy NT, Minh DL. Size effect on the structural and magnetic properties of nanosized perovskite $LaFeO_3$ prepared by different methods, Adv. Mater. Sci. Eng. 2012;1155(1-6):380306.
13. Kumar M, Srikanth S, Ravikumar B, Alex TC, Das SK. Synthesis of pure and Sr-doped $LaGaO_3$, $LaFeO_3$ and $LaCoO_3$ and Sr, Mg-doped $LaGaO_3$ for ITSOFC application using different wet chemical routes, Mater. Chem. Phys. 2009 Feb 15;113(2-3):803-15.
14. Gosavi PV, Biniwale RB. Pure phase $LaFeO_3$ perovskite with improved surface area synthesized using different routes and its characterization, Mater. Chem. Phys. 2010 Jan 15;119(1-2):324-9.
15. Yang Z, Huang Y, Dong B, Li HL. Controlled synthesis of highly ordered $LaFeO_3$ nanowires using a citrate-

based sol–gel route, Mater. Res. Bull. 2006 Feb 2;41(2):274-81.
16. Costa ACFM, Morelli MR, Kiminami RHGA. Combustion Synthesis Process of Nanoceramics. Handbook of Nanoceramics and Their Based Nanodevices. In:Tseng-Yuen Tseng and Hari Singh Nalwa (Eds.). 2009;1:375-392.
17. Jain SR, Adiga KC, Pai Verneker V. Thermodynamic, structural and magnetic studies of $NiFe_2O_4$ nanoparticles prepared by combustion method: Effect of fuel. Combust. Flame. 1981;40:71-79.
18. Larson AC, Von Dreele RB. General Structure Analysis System (GSAS), Los Alamos National Laboratory Report LAUR; c2004, p. 86-748.
19. Klug HP, Alexander LE. X-ray Diffraction Procedures for Polycrystalline and Amorphous Materials. Wiley, New York; c1997, p. 637.
20. Prado-Gonjal J, Arévalo-López ÁM, Morán E. Microwave-assisted synthesis: A fast and efficient route to produce $LaMO_3$ (M = Al, Cr, Mn, Fe, Co) perovskite materials. Mater. Res. Bull. 2011;46(2):222-230.
21. Wang J, Liu Q, Xue D, Li F. Synthesis and characterization of $LaFeO_3$ nano particles. J. Mater. Sci. Lett. 2002;21(13):1059-1062.
22. Kumar M, Srikanth S, Ravikumar B, Alex TC, Das SK. Synthesis of pure and Sr-doped $LaGaO_3$, $LaFeO_3$ and $LaCoO_3$ and Sr, Mg-doped $LaGaO_3$ for ITSOFC application using different wet chemical routes. Mater. Chem. Phys. 2009;113(2-3):803-815.
23. Köferstein R, Ebbinghaus SG. Synthesis and characterization of nano-$LaFeO_3$ powders by a soft-chemistry method and corresponding ceramics. Solid State Ionics. 2013;231:43-48.
24. Rezlescu N, Rezlescu E, Popa PD, Popovici E, Doroftei C, Ignat M. Preparation and characterization of spinel-type $MeFe_2O_4$(Me = Cu, Cd, Ni and Zn) for catalyst applications. Mat Chem Phys. 2013;137(3):922-927.
25. Rezlescu N, Rezlescu E, Popa PD, Popovici E, Doroftei C, Ignat M. Preparation and characterization of spinel-type $MeFe_2O_4$(Me = Cu, Cd, Ni and Zn) for catalyst applications. Mat Chem Phys. 2013;137(3):922-927.
26. Shter GE, Schwartzman AR, Grader GS.) Interrelation of calcination temperature, surface area and densification of oxalate-derived YBCO. Appl Super Cond. 1995;3(11-12):543-550.